THE JOURNAL OF PHYSICAL CHEMISTRY B

Article

pubs.acs.org/JPCB

Understanding Protein Diffusion in Polymer Solutions: A Hydration with Depletion Model

Xiaoqing Feng,[†] Anpu Chen,[†] Juan Wang,[†] Nanrong Zhao,*[,†] and Zhonghuai Hou*[,‡]

[†]College of Chemistry, Sichuan University, Chengdu 610064, China

[‡]Hefei National Laboratory for Physical Sciences at the Microscale & Department of Chemical Physics, University of Science and Technology of China, Hefei, Anhui 230026, China

ABSTRACT: Understanding the diffusion of proteins in polymer solutions is of ubiquitous importance for modeling processes in vivo. Here, we present a theoretical framework to analyze the decoupling of translational and rotational diffusion of globular proteins in semidilute polymer solutions. The protein is modeled as a spherical particle with an effective hydrodynamic radius, enveloped by a depletion layer. On the basis of the scaling formula of macroscopic viscosity for polymer solutions as well as the mean-field theory for the depletion effect, we specify the space-dependent viscosity profile in the depletion zone. Following the scheme of classical fluid mechanics, the hydrodynamic drag force as well as torque exerted to the protein can be numerically evaluated, which then allows us to obtain the translational and rotational diffusion coefficients. We have applied our model to study the diffusion of proteins in two particular polymer solution systems, i.e., poly(ethylene glycol) (PEG) and dextran. Strikingly, our theoretical results can reproduce the experimental results quantitatively very well, and fully reproduce the decoupling between translational and rotational diffusion observed in the experiments. In addition, our model facilitates insights into how the effective hydrodynamic radius of the protein changes with polymer systems. We found that the effective hydrodynamic radius of proteins in PEG solutions is nearly the same as that in pure water, indicating PEG induces preferential hydration, while, in dextran solutions, it is generally enhanced due to the stronger attractive interaction between protein and dextran molecules.

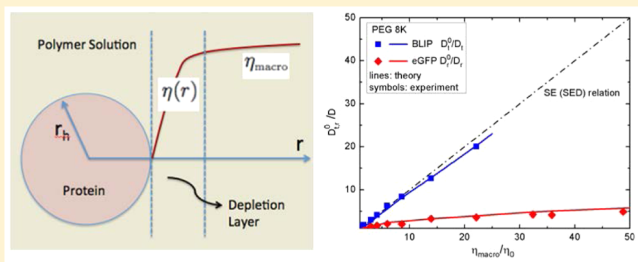

■ INTRODUCTION

The transport property of proteins in complex fluids is a benchmark problem of modeling processes likely to regulate cellular functions such as signal transduction,[1,2] self-assembly of supramolecular structures,[3] kinetics of reaction,[4] gene transcription,[5] and so on. A better understanding of this problem would also be beneficial to several important fields of studies across disciplines ranging from biophysics, materials science, and even drug delivery. In particular, in biophysics, there is a growing interest to understand how proteins move through crowded cytoplasmic environments. Synthetic polymers such as polyethylene glycol (PEG), ficoll, dextran, and poly(vinyl alcohol) are commonly used as a means to mimic molecular crowding in the cell, which facilitates experimental studies in vitro.[6−10] Fluorescence correlation spectroscopy and fluorescence anisotropy are most popular in this area of research, by the aid of which the translational and rotational diffusion of proteins in semidilute polymer solutions and their contributions to the diffusion-controlled protein−protein association kinetics have been widely investigated.[7,11−15] Nevertheless, some fundamental aspects are still lacking and a comprehensive understanding is definitely desirable.

In pure solvent or simple solutions with a low-molecular crowding agent like glycerol, experiments have found[16−18] that the translational diffusion coefficient D_t can be well predicted by the traditional Stokes−Einstein (SE) relation, $D_t = k_BT/6\pi\eta_{macro}r_h$, and the rotational diffusion coefficient by the Stokes−Einstein−Debye (SED) relation, $D_r = k_BT/8\pi\eta_{macro}r_h^3$, with η_{macro} being the macroviscosity of the solution, r_h the hydrodynamic radius of diffusing species, T the temperature, and k_B the Boltzmann constant. The validity of the SE (or SED) relation requires a continuous and homogeneous solvent condition. As the probe size becomes smaller or the crowding agent becomes larger, this condition in general does not hold. Extensive experimental studies have revealed that the diffusion coefficients of small nanoparticles and small proteins in polymer solutions will seriously deviate from SE and SED relations even up to several orders of magnitude.[16,17,19−22] The deviation is almost negative; i.e., the decrease in diffusion with increased viscosity is less than predicted, and furthermore, the negative deviation increases with increasing polymer concentration and molecular weight. Great efforts have been made for a quantitative strategy to evaluate the diffusion coefficients in polymer solutions at all length scales. In particular, Holyst et al.[10,23−28] studied systematically the translational diffusion of nanoparticles and proteins in semidilute polymer solutions by

Received: June 20, 2016
Revised: September 4, 2016
Published: September 6, 2016

DOI: 10.1021/acs.jpcb.6b06248
J. Phys. Chem. B 2016, 120, 10114−10123

experiments. They proposed interesting and inspiring scaling relations for translational diffusion coefficients; namely, if one replaces the macroscopic viscosity by a so-called length-scale-dependent microscopic viscosity $\eta_{\rm micro}$ which may depend on the probe size, the SE relation could be valid for all length scales. This provides an explicit relationship between the diffusion coefficient and simple parameters describing the structure of the system: radius of diffusing species, hydrodynamic radius of polymer molecules, and correlation length of polymer solutions. Similarly, Lavalette et al.[9,29] suggested a power law form of microscopic viscosity for rotational diffusion of proteins in a macromolecular environment, to replace the linear viscosity dependence of the SED relation. The exponent of the power law is less than one, which indicates the consequence of nonhomogeneity due to the fact that the protein experiences only a fraction of the hydrodynamic interactions of macromolecular cosolvents. Alternatively, Fan et al.[30−32] proposed a fluid mechanics approach to investigate the length-scale-dependent viscosity for both translational and rotational diffusion coefficients of a sphere in polymer solutions.

While most studies up to now have mainly focused on how translational or rotational diffusion of a solute in complex fluids deviates from the SE (or SED) relation, recently, a very interesting *decoupling* phenomenon between the translational and rotational diffusion has drawn some new attention. Namely, it was found experimentally[7,12,13,33,34] that, for diffusion of proteins in polymer solutions, large deviations from the traditional SED relation are observed for the rotational diffusion with an increase of the bulk concentration of polymer solution, while the SE relation for the translational diffusion remains well satisfied. The understanding of such a decoupling phenomenon can be very important, for example, to illustrate the separate contributions of translational and rotational diffusion to important processes in vivo such as protein−protein association kinetics.[7,12,13,35] To the best of our knowledge, however, such an understanding is still lacking.

In the present work, we have addressed such an issue by proposing a theoretical framework, by modeling the protein as a spherical particle with an effective hydrodynamic radius $r_{\rm h}$ enveloped by a depletion layer. Our idea is that the decoupling is mainly due to the nonhomogeneous viscosity profile in the depletion zone, which would influence the translational and rotational diffusion in quantitatively different ways. Due to depletion effects, the polymer volume fraction is not homogeneous around the protein, which can be described by a distance-dependent profile $\phi(r)$, where r denotes the distance from the center of the protein. We then adopt the scaling theory[27,28] between the macroscopic viscosity and the polymer concentration which has been proven to be valid for a wide range of concentrations ranging from dilute to semidilute regimes, to get the viscosity profile $\eta(r)$. Combining this viscosity profile with fluid mechanics, we can then calculate the translational as well as rotational diffusion coefficients $D_{\rm t}$ and $D_{\rm r}$, respectively. Such a framework is quite clear-cut in physics, given that the protein can be regarded averagely as a spherical particle with effective hydrodynamic radius $r_{\rm h}$, which serves as the only fitting parameter in the present model. We apply our model to two typical systems, one for diffusion of globular proteins in PEG solutions and the other for diffusion in dextran solutions. Strikingly, our theoretical results can reproduce the experimental results *quantitatively* very well, and fully reproduce the decoupling between translational and rotation diffusion observed in the experiments. Moreover, we found that, in the case of PEG solutions, the hydrodynamic radius $r_{\rm h}$ is nearly the same as that in the pure water solvent, indicating the protein is surrounded by water molecules as it moves in the PEG solutions. This result agrees with the work of Bhat and Timasheff[36] who showed that PEG induces preferential hydration of proteins. However, in the case of dextran solutions, the protein is likely to possess a higher hydrodynamic radius due to the probable stronger attractive interaction between protein and dextran molecules.

The paper is organized as follows. First, we introduce our model and method, including the nonuniform concentration and viscosity profiles due to the depletion effect and a brief revisit of derivation for diffusion coefficients based on fluid mechanics. Second, we numerically calculate the translational and rotational diffusion coefficients for proteins in two types of polymer solutions. Comparison with the experiments will be made and the uncoupling between two diffusion motions as well as the effective hydrodynamic radius will be addressed. At last, we conclude the paper.

■ MODEL AND METHOD

Basic Modeling. We model the protein as a spherical particle with an effective hydrodynamic radius $r_{\rm h}$, enveloped by a depletion layer wherein the concentration and viscosity are space-dependent, as depicted in Figure 1. For simplicity, we adopt the following theoretical form within the mean-field approximation to describe the volume fraction profile in terms of the radial distance r ($r_{\rm h} \le r < \infty$) in the depletion zone[30,37]

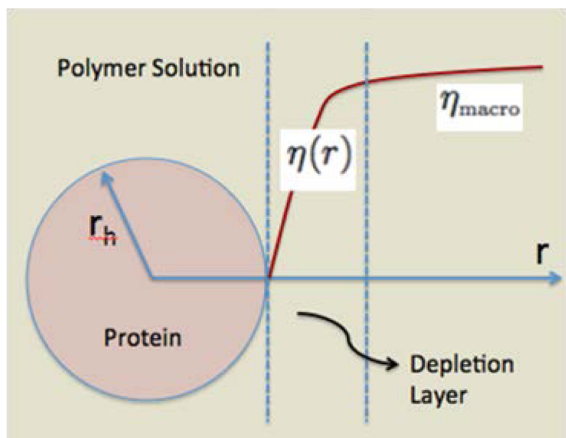

Figure 1. Schematic of the model.

$$\phi(r) = \phi_{\rm b}\left[r - r_{\rm h} + \tanh\left(\frac{r - r_{\rm h}}{\delta}\right)\right]^2 / r^2 \tag{1}$$

This expression is actually an extension of the exact form in the limit of dilute solution and flat geometry to spheres in semidilute polymer solutions. In eq 1, $\phi_{\rm b}$ is the bulk volume fraction. δ is a polymer solution parameter which has a meaning of the depletion thickness near a flat wall in semidilute solutions, given by

$$\frac{1}{\delta^2} = \frac{1}{{\delta_0}^2} + \frac{1}{{\xi_{\rm FH}}^2} \tag{2}$$

where δ_0 is proportional to the gyration radius of the polymer, to be $\delta_0 = \frac{2}{\sqrt{\pi}}R_{\rm g}$. $\xi_{\rm FH}$ is basically the correlation length of the

DOI: 10.1021/acs.jpcb.6b06248
J. Phys. Chem. B 2016, 120, 10114−10123

polymer solution. In the mean-field picture with potential described by the Flory−Huggins field,[38,39] it takes the specific form of $\xi_{FH}^{-2} = -3[\ln(1-\phi_b) + 2\chi\phi_b]\sigma^{-2}$, with χ being the solvency and σ the statistical segment length of polymer chains. In the present work, we limit ourselves to a good solvent situation, i.e., $\chi = 0$.

One should note that the basic model introduced here highlights the crucial role of the depletion layer, which certainly has its main range of validity. As mentioned in the Introduction, the main goal of this work is to understand the interesting decoupling phenomenon between the translational and rotational diffusion, wherein SE holds for D_t while SED fails for D_r. In addition, the rotational diffusion is much faster than that predicted by the SED relation, indicating a relatively small viscosity around the probe particle. It has been reported that this depletion effect is the strongest for $r_h \simeq R_h$, where R_h is the hydrodynamic radius of the polymer molecule. For both $r_h < R_h$ and $r_h > R_h$, the depletion effect might be neglected, and the length-scale-dependent viscosity model has been proposed to describe translational diffusion of particles in polymer solutions. One should note, however, the length-scale-dependent viscosity model[23,26,28] for translational motion cannot account for the decoupling between D_t and D_r. In real complex polymer solutions, permanent cross-links and strong entanglements may exist such that the protein diffusion is influenced by many factors, including hopping and network relaxation besides simple hydrodynamic forces. Any rheological phenomenon affecting the macroviscosity that arises on a length scale above the hydrodynamic screening length of a given semidilute solution (i.e., from topological, possibly transient connectivity effects) cannot be included in the present model. Therefore, our model may apply to the diffusion of proteins with $r_h \simeq R_h$, in polymer solutions without strong topological effects or permanent links.

Space-Dependent Viscosity. Depletion leads to a volume fraction profile given by eq 1. Correspondingly, the viscosity in the vicinity of the protein surface is also nonhomogeneous, which should vary from the bare viscosity η_0 to the bulk macroviscosity η_{macro}. In order to quantitatively characterize the viscosity distribution in the depletion layer, we note that Holyst et al.[27,28] recently proposed a phenomenological scaling theory for the relationship between macroviscosity and concentration for polymer solutions, given by

$$\eta_{macro} = \eta_0 \exp\left[\left(\frac{\gamma}{RT}\right)\left(\frac{R_h}{\xi}\right)^{\beta}\right] \tag{3}$$

where γ and β are system-dependent parameters. R_h is the polymer hydrodynamic radius, and ξ is the correlation length of the polymer solution which will decrease with the concentration obeying the scaling relation as follows

$$\xi = R_g\left(\frac{\phi_b}{\phi^*}\right)^{-3/4} \tag{4}$$

with ϕ^* being the overlap volume fraction of the polymer solution from the dilute to semidilute regime given by

$$\phi^* = \frac{3M_w}{4\pi d N_A {R_g}^3} \tag{5}$$

with M_w being the polymer molecular weight, d the polymer mass density, and N_A the Avogadro constant. Note that, in the work of Fan et al.,[30,40] the dependence of η_{macro} on the bulk volume fraction ϕ_b was introduced via the Huggins' or Martins' theoretical formula. We use eq 3 here because it was shown to be valid for semidilute polymer solutions, even in the entangled region.

Combining eqs 1, 3, as well as 4, we get the appropriate viscosity profile $\eta(r)$ in the depletion layer, in the form of

$$\eta(r) = \eta_0 \exp\left[\left(\frac{\gamma}{RT}\right)\left(\frac{R_h}{R_g}\right)^{\beta}\left(\frac{\phi(r)}{\phi^*}\right)^{3\beta/4}\right] \tag{6}$$

The nonhomogeneity of viscosity will induce deviations from SE and SED relations for translational and rotational diffusion coefficients, respectively, and the above viscosity profile is just the starting point to quantitatively estimate these deviations on the basis of fluid mechanics as described below.

We would like to emphasize here that eq 6 is one of the main starting points of our work. One should note that the space-dependent viscosity $\eta(r)$ in eq 6 actually corresponds to macroscopic viscosity, rather than the so-called microviscosity which might be dependent on the length scale of the solute size. Actually, Holyst et al. had investigated in very much detail the length-scale-dependent viscosity that is experienced by the diffusing species in complex fluids such as polymer solutions. In the present work, the space-dependent viscosity $\eta(r)$ accounts for the nonhomogeneous macroscopic viscosity in the depletion layer due to the space-dependent volume fraction profile $\phi(r)$ given by eq 1. On the basis of such a viscosity profile, one is thus able to derive the translational and rotational diffusion coefficients of the protein, here modeled as a spherical particle with effective hydrodynamic radius r_h, by using standard methods in fluid mechanics but now with inhomogeneous viscosity.

Here, we would like to point out a subtle issue regarding the viscosity profile $\eta(r)$ given by eq 6. The volume fraction profile $\phi(r)$ in eq 1 is actually bounded, which should not diverge. Therefore, if the correlation length ξ obeys the scaling law in eq 3, the viscosity profile $\eta(r)$ would also be bounded. However, for some limiting cases like a hydrogel, the zero-shear macroviscosity η_{macro} may diverge, such that a probe particle with $r_h \to \infty$ would become jammed. In such a situation, either eq 3 or 4 may fail and new theory may be necessary. We note that such a theory had been worked out by Rubinstein and coworkers.[41] For the systems considered in the present work, the PEG and dextran solutions, eq 3 works very well as shown in the literature[27,28] and Figure 4 below.

Fluid Mechanics with $\eta(r)$. The basic procedures to calculate the translational and rotational diffusion coefficients D_t and D_r can be outlined as follows. The fluid field $\mathbf{v}(r)$ around the particle is incompressible and obeys the Navier−Stokes equations but now with space-dependent viscosity $\eta(r)$. By solving the field equations with proper boundary conditions, one can get the pressure and the shear stress of the polymer solution at the protein surface. This allows us to calculate the drag force F and the shear-induced torque Γ exerted on the protein. Assuming protein moves with translational velocity U and rotates with angular velocity Ω, D_t and D_r will correspondingly follow[42] $D_t = Uk_BT/F$ and $D_r = \Omega k_BT/\Gamma$. The readers may turn to ref 30 for technical details, and here we will only quote the final results for simplicity.

Consequently, the translational diffusion coefficient D_t is given by

DOI: 10.1021/acs.jpcb.6b06248
J. Phys. Chem. B 2016, 120, 10114−10123

$$\frac{D_t^0}{D_t} = \left(\frac{r_h}{r_h^0}\right)\left[\frac{4}{9} + \frac{4}{9}r_h^{2}f''(r_h) - \frac{2}{9}r_h^{3}f'''(r_h)\right] \tag{7}$$

where $D_t^0 = k_BT/6\pi\eta_0 r_h^0$ is the traditional diffusion coefficient of the protein in pure solvent. Here r_h^0 is the hydrodynamic radius of protein in pure solvent, which might be different from the effective hydrodynamic radius r_h for a protein diffusing in polymer solutions as depicted in Figure 1. $f''(r_h)$ and $f'''(r_h)$ denote the second- and third-order derivatives of the function $f(r)$ at $r = r_h$. This function $f(r)$ describes the radius-dependent part of the Stokes stream function and satisfies the following fourth-order ordinary differential equation

$$\frac{d^4f}{dr^4} + \frac{2\eta'}{\eta}\frac{d^3f}{dr^3} - \left(\frac{4}{r^2} + \frac{2\eta'}{r\eta} - \frac{\eta''}{\eta}\right)\frac{d^2f}{dr^2} + \left(\frac{8}{r^3} - \frac{2\eta'}{r^2\eta} - \frac{2\eta''}{r\eta}\right)\frac{df}{dr} - \left(\frac{8}{r^4} - \frac{8\eta'}{r^3\eta} - \frac{2\eta''}{r^2\eta}\right)f = 0 \tag{8}$$

where η' and η'' denote the first- and second-order derivatives of $\eta(r)$ with respect to r, respectively. Given the viscosity profile $\eta(r)$ as input, this equation for $f(r)$ can be solved numerically with certain boundary conditions. For a quiescent fluid, we apply no-slip boundary conditions at the protein surface, i.e., $f(r = r_h) = -\frac{1}{2}$, $f'(r = r_h) = -1/r_h$, and vanishing far-field conditions, i.e., f/r^2 and f'/r go to zero as $r \to \infty$.

Similarly, one can obtain the rotational diffusion coefficient D_r according to

$$\frac{D_r^0}{D_r} = \frac{1}{3}\left(\frac{r_h}{r_h^0}\right)^3[1 - r_h\omega'(r_h)] \tag{9}$$

where $D_r^0 = k_BT/8\pi\eta_0 r_h^{0\,3}$ is the rotational diffusion coefficient of the protein in pure solvent. $\omega'(r_h)$ denotes the derivative of the radial function $\omega(r)$ with respect to r at $r = r_h$. $\omega(r)$ satisfies the following differential equation

$$\frac{d^2\omega}{dr^2} + \left(\frac{2}{r} + \frac{\eta'}{\eta}\right)\frac{d\omega}{dr} - \left(\frac{2}{r^2} + \frac{\eta'}{r\eta}\right)\omega = 0 \tag{10}$$

This equation can be solved numerically with no-slip boundary condition $\omega(r_h) = 1$ and vanishing far-field condition $\omega(r \to \infty) = 0$. It is noticeable that the no-slip boundary condition is in general not applicable for very small diffusing probes. In the present study, as we mentioned above, we mainly deal with proteins with moderate size, i.e., $r_h \simeq R_h$, such that no-slip boundary condition is reasonable.

We are now ready to study the diffusion coefficients of a given protein in specific polymer solutions. As already mentioned in the Introduction, we are interested in the phenomenon that the SE relation holds for D_t, while in the same system SED deviates largely for D_r. We believe that this deviation mainly results from the inhomogeneous viscosity in the depletion layer, ranging from η_0 of the pure solvent to η_{macro} for the bulk solution. In this scheme, the protein is treated as a sphere particle with an effective hydrodynamic radius r_h, which is the only parameter for the protein that enters into the volume fraction profile $\phi(r)$ given by eq 1 and henceforth the viscosity profile $\eta(r)$ given by eq 6. All of the other parameters that enter $\eta(r)$, such as ϕ^*, R_h, R_g, β, and γ, are determined by the polymer solution, in which the crossover volume fraction ϕ^*, the polymer hydrodynamic radius R_h, and the gyration radius R_g depend on the polymer molecular weight M_w. Therefore, a general discussion of the above framework may not be helpful and we would like to apply it to specific real systems where experimental data are available. This will be presented in the next section for two systems: one is for diffusion of globular proteins in poly(ethylene glycol) (PEG) solutions, and the other is for protein diffusion in dextran solutions.

■ RESULTS AND DISCUSSION

Protein Diffusion in PEG Solutions. In this section, we proceed to quantitatively study the diffusion coefficients for protein diffusion in PEG solutions. We consider the diffusion of two types of globular protein: β-lactamase inhibitor protein (BLIP) and a green fluorescent protein mutant (eGFP) in solutions of PEG with different molecular weights and varying concentrations. The hydrodynamic radii of the proteins in pure water, r_h^0, can be estimated to be 2.2 nm for BLIP and 2.5 nm for eGFP, on the basis of the fact that the hydrodynamic volume for a globular protein is nearly twice its crystal volume.[43] Experimentally, translational and rotational diffusion of proteins can be obtained by using fluorescence correlation spectroscopy and fluorescence anisotropy, respectively. The experimental data for D_t and D_r quoted in the present work are obtained from refs 7 and 12.

To this end, we first need to determine the parameters that enters $\eta(r)$, namely, ϕ^*, R_h, R_g, β, and γ. Here, ϕ^* is given by eq 5. R_h and R_g depend on the molecular weight according to $R_h = 0.0145M_w^{0.571}$ and $R_g = 0.0215M_w^{0.583}$ for PEG systems.[27,44] β is a relatively universal parameter for polymer solutions depending on whether the system is entangled or not. It is widely accepted that $\beta \simeq 1.29$ in the nonentangled regime and $\beta \simeq 0.78$ in the entangled regime. The crossover from nonentangled to entangled regime takes place at the volume fraction ϕ_e for which the hydrodynamic radius of the polymer R_h is just equal to the correlation length ξ given by eq 4, such that $\phi_e = (R_h/R_g)^{-4/3}\phi^*$. γ is estimated by fitting experimental data, which has been reported to be 4.0 kJ/mol for PEG solutions.[27]

In the present work, PEG samples of two different molecular weights 1 kg/mol (PEG 1K) and 8 kg/mol (PEG 8K) are investigated. The corresponding basic parameters including the overlap volume fraction ϕ^*, the onset volume fraction for the entangled regime ϕ_e, the hydrodynamic radius R_h, and the gyration radius R_g of PEG are listed in Table 1. In addition, for the PEG system, the mass density is $d = 1126$ kg/m^3 and the statistical segment length is $\sigma = 0.7$ nm.[45] Besides these system parameters, the bulk volume fraction ϕ_b of the polymer solution is a variable which also determines the viscosity profile $\eta(r)$ through the volume fraction function $\phi(r)$ given by eq 1.

Table 1. Basic Parameters of PEG Solutions

PEG M_w (kg/mol)	ϕ^*	ϕ_e	R_h (nm)	R_g (nm)
1	0.20	0.38	0.75	1.21
8	0.042	0.083	2.45	4.05

Second, we must specify the effect hydrodynamic radius of proteins r_h, which is necessary to determine the volume fraction profile $\phi(r)$ and henceforth the viscosity function $\eta(r)$. Note that the effective hydrodynamic radius r_h in complex solutions should be in general different from the hydrodynamic radius in pure water r_h^0. In fact, r_h has to be a fitting parameter in our

DOI: 10.1021/acs.jpcb.6b06248
J. Phys. Chem. B 2016, 120, 10114−10123

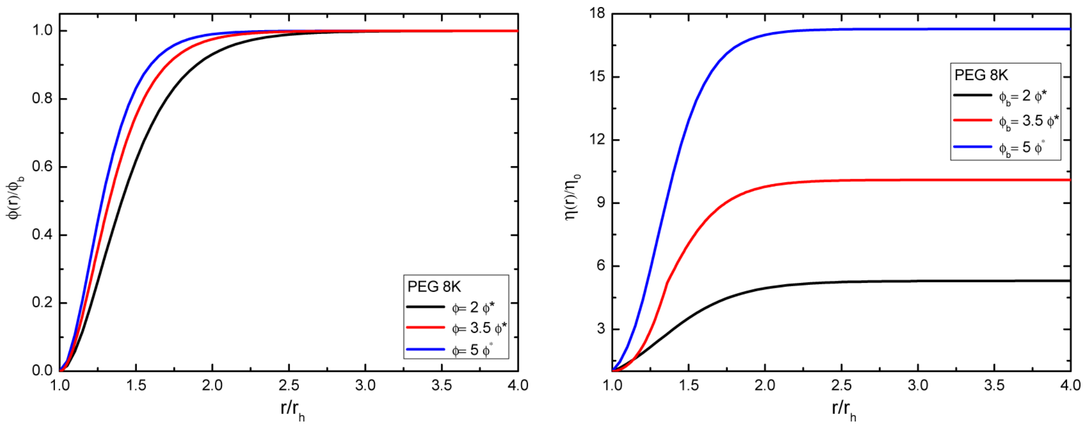

Figure 2. Space-dependent volume fraction $\phi(r)$ as well as the local viscosity profiles $\eta(r)$, for BLIP in PEG 8K solutions with different bulk volume fraction ϕ_b.

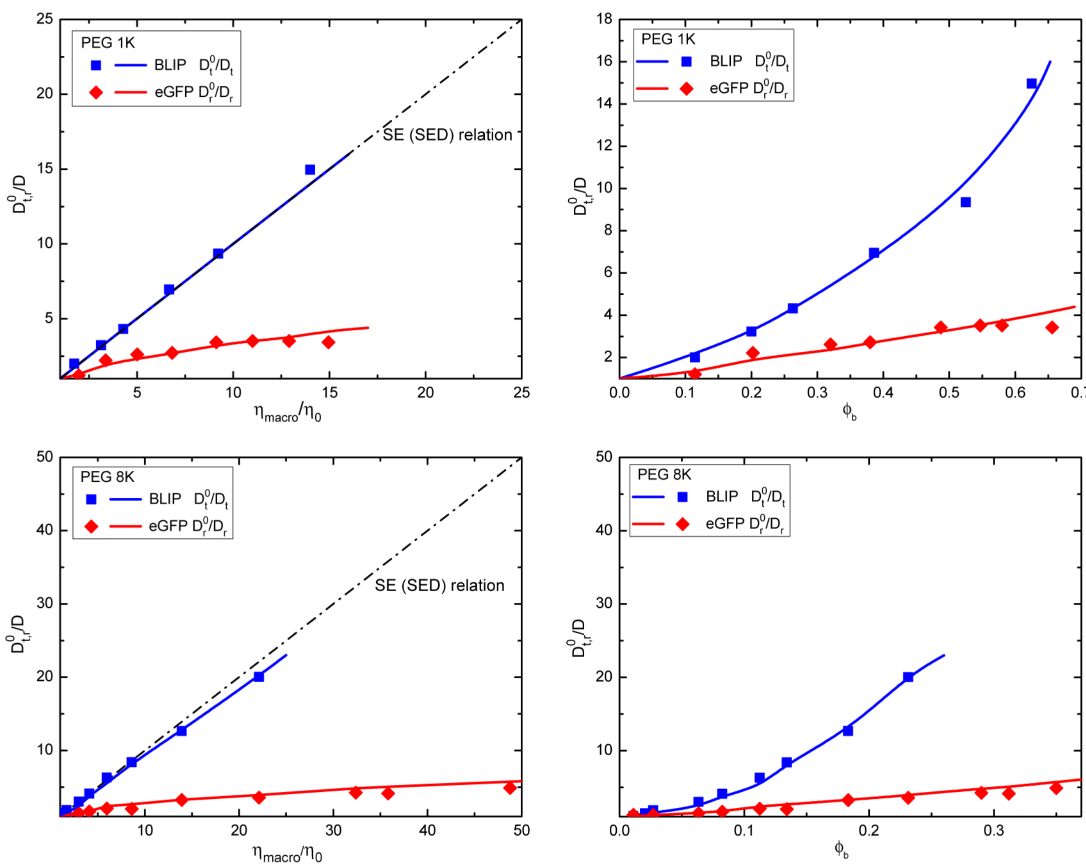

Figure 3. Dependence of relative translational diffusion coefficient D_t^0/D_t of BLIP (blue lines) and relative rotational diffusion coefficient D_r^0/D_r of eGFP (red lines) on relative viscosity η_{macro}/η_0 (left column) and on bulk volume fraction ϕ_b (right column) in PEG 1K (upper) and PEG 8K (bottom) solutions. Symbols are experimental data reproduced from refs 7 and 12 for comparison.

theoretical formalism. For PEG systems, recall that there was a preferential hydration picture proposed by Bhat and Timasheff.[36] The basic physics being shown is that the attraction between the protein and PEG molecules is weaker than the interaction between the protein and water molecules. Therefore, the protein molecule becomes preferentially hydrated similar to its behavior in pure water solvent, and then diffuses in PEG solutions. In this sense, the hydrodynamic radius of the protein in PEG solution possibly stays nearly the same as that in water. Surely, this picture will break down if the protein has stronger attractive interactions with the polymer chains, which would definitely enhance the protein effective hydrodynamic radius. Indeed, as we will show in the next subsection, higher effective hydrodynamic radius might be realized, for example, in dextran solutions. However, for PEG solutions, it seems reasonable for us to propose an ansatz that the effective hydrodynamic radius of protein diffusion in PEG solutions is *nearly the same* as that in the pure water solvent. With the above arguments, the effective hydrodynamic radius, $r_h \simeq r_h^0$ for the two proteins BLIP and eGFP considered here, is set to be 2.2 and 2.5 nm, respectively.

DOI: 10.1021/acs.jpcb.6b06248
J. Phys. Chem. B 2016, 120, 10114−10123

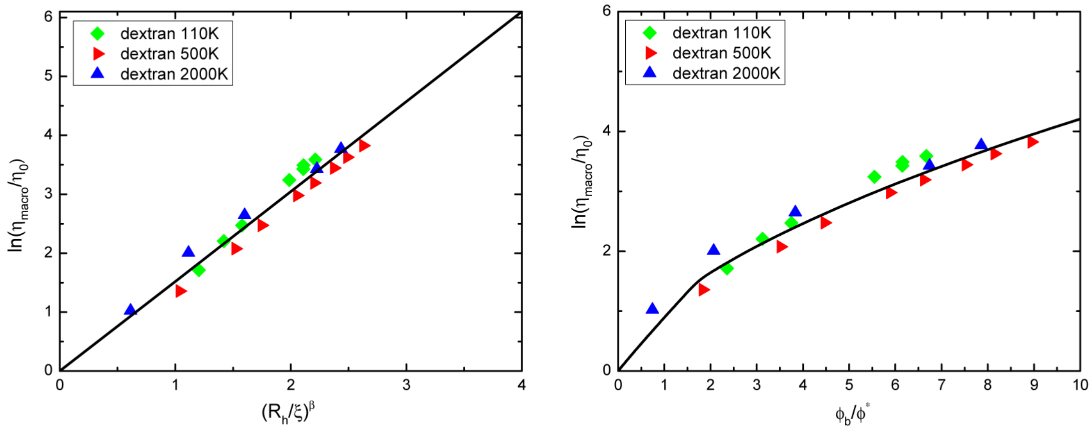

Figure 4. Relative macroscopic viscosity for dextran solutions plotted according to the scaling equation (3) (lines), with β equal to 1.29 for $R_h/\xi \le 1$ and 0.78 for $R_h/\xi > 1$, and $\gamma \simeq 3.5$ kJ/mol by a best fitting to experimental data (symbols) from ref 9.

Now we are ready to calculate diffusion coefficients D_t and D_r by using eqs 7−10. To this aim, it is necessary to be specific about the space-dependent volume fraction $\phi(r)$ as well as the local viscosity profile $\eta(r)$; see Figure 2 as an illustration. We mainly focus on how these diffusion coefficients change with the bulk volume fraction ϕ_b and thus with the macroviscosity η_{macro} of PEG solutions. The results are shown in Figure 3 for the diffusion of BLIP and eGFP in PEG 1K and PEG 8K solutions, respectively. In the experiments, translational diffusion was measured for BLIP and rotational diffusion was measured for eGFP. The vertical axis is the ratio of the diffusion coefficients in PEG solutions to that in pure water $D^0_{t,r}/D_r$. The solid lines are obtained from our theory. The symbols are the experimental data from refs 7 and 12. The dash-dotted line is the SE and SED prediction, where the relative diffusion coefficient is linearly proportional to the relative viscosity.

Surprisingly, our theory reproduces the experimental results very well, not only qualitatively but also quantitatively. The theory excellently demonstrates that the SE relation holds good for the translational diffusion, while SED breaks down apparently for rotational diffusion. Such excellent consistency between theory and experiment also indicates that our model has caught the main physics of the problem considered; i.e., the inhomogeneous viscosity profile due to the depletion effect can be the very reason for the decoupling between translational and rotational diffusion. Quantitative agreements also indicate that the ansatz we proposed about the preferential hydration of protein is indeed applicable in the PEG solution.

In a recent paper,[23] Holyst and co-workers have systematically studied the translational diffusion of proteins of different sizes in PEG solutions with different molecular weights. They found that, while probes with large size obey the SE relation, proteins with small size show apparent violations of the relation. They then introduced a size-dependent nanoviscosity $\eta(a)$, where a denotes the probe size, which showed a collapsed scaling form with a crossover length to be R_g. One may ask whether we can use the present model to account for the size dependence of D_t. Unfortunately, as already mentioned in the Model and Method section, the model highlights the depletion effect which becomes significant for $r_h \simeq R_h$. For small proteins, the SE relation is already violated for translational diffusion, indicating that some other effects must be taken into account. We note that some recent theoretical work using mode coupling theory[45] can help in understanding this problem, wherein binary collision and density fluctuation on the short length scale come into play. Such effects rather than simple hydrodynamics go beyond the scope of the current model. Actually, the fact that the small protein diffuses much faster than the SE prediction indicates that the nanoviscosity, "felt" by the protein, is actually much smaller than the macroviscosity in the bulk. Mapping to our model, it seems that the protein should experience a much thicker depletion layer, wherein the concentration as well as viscosity are much smaller than in the bulk. If we apply our model to the data in ref 23 for small proteins like 3.1 nm lysozyme in PEG 20K, an apparent underestimation of D_t would be observed (not shown). If one further allows the depletion layer depth δ to be changed as a parameter δ^{eff} to fit the experimental data, it will decrease monotonically with the bulk concentration.

Protein Diffusion in Dextran Solutions. We now try to use the above scheme to study the diffusion of proteins in another polymer solution system, the dextran solution. The experimental results are obtained from ref 9 for diffusion of earthworm (Lumbricus terrestris) hemoglobin (EW-Hb) and of a fragment thereof (F(EW-Hb)). The hydrodynamic radii of EW-Hb and F(EW-Hb) in pure water r^0_h are 13.4 and 5.7 nm, respectively.

For dextran, the hydrodynamic and gyration radii depend on its molecular weight M_w via[46] $R_h = 0.0488 M_w^{0.437}$ and $R_g \simeq 1.5 R_h$.[26] Concerning the relationship between macroviscosity and concentration of dextran solutions, we suppose eq 3, which has shown its validity sufficiently in PEG solutions, also works for dextran solutions. Figure 4 is a plot of this equation as well as the corresponding experimental data (symbols).[9] The validity of this scaling expression has been well demonstrated by this figure. Here, the parameter β is chosen to be the same as that of PEG, depending on whether the solution is entangled or not. While another important empirical parameter γ is obtained by fitting the experimental data, we have $\gamma \simeq 3.5$ kJ/mol for dextran solutions. In order to compare our theory with experimental work, we will correspondingly investigate proteins EW-Hb and F(EW-Hb) in dextran samples with three different molecular weights 110, 500, and 2000 kg/mol. The required basic parameters for calculating the diffusion coefficients are listed in Table 2, including the overlap volume fraction ϕ^*, the onset volume fraction for the entangled regime ϕ_e, the hydrodynamic radius R_h, and the gyration radius R_g for different dextran samples. Besides, for dextran, we have the mass density[47] $d = 1600$ kg/m^3 and the statistical segment length[48] $\sigma = 1.2$ nm.

DOI: 10.1021/acs.jpcb.6b06248
J. Phys. Chem. B 2016, 120, 10114−10123

Table 2. Basic Parameters of Dextran Solutions

dextran M_w (kg/mol)	ϕ^*	ϕ_e	R_h (nm)	R_g (nm)
110	0.017	0.029	7.79	11.68
500	0.011	0.018	15.10	22.64
2000	0.0069	0.012	27.67	41.50

One should note here that the results for macroviscosity in ref 9 had been measured by capillary viscosimetry using simple Ubbelohde setups. Under these conditions, for the highly nonlinear entangled case, this method does not provide the macroscopic zero-shear viscosity in the linear viscoelastic regime but the shear-thinning limit, in which structural changes such as flow-induced disentanglement may occur. Nevertheless, the macroviscosity η_{macro} in the scaling form given by eq 3 actually corresponds to the zero-shear one. In general, one should do actual rheology by using a proper capillary system with potentially low flow rate to get this macroviscosity such as those done in ref 23. Therefore, it is interesting that the data shown in Figure 4 can be fitted so well by the scaling formula, eq 3. Possibly, this reported high-shear viscosity may indeed be of relevance on the shorter length scale of protein diffusion, but the relation to the true macroviscosity is not clear in that case. In this sense, the η_{macro} shown in Figure 1 might be better illustrated as η_{meso}, which is a mesoscopic-length-scale viscosity and not necessarily equal to the zero-shear bulk macroviscosity when strong entanglement or cross-linking effects are active. It is also interesting to ask why the scaling exponent shown in eq 3 does seem to work for this η_{meso}. For our purpose, however, we only require that eq 3 and thus eq 6 give an accurate functional form of the space-dependent viscosity profile $\eta(r)$ for succeeding fluid-dynamics analysis.

As already discussed in the last subsection, to apply our modeling, one must specify the "effective" hydrodynamic radius r_h of the protein in the solution. For the PEG system studied above, one expects preferential hydration of the protein due to the relatively weak attraction between protein and PEG molecules, such that r_h may be nearly the same as r_h^0 in the pure water solvent. We have also demonstrated that such a picture really works well for diffusion of BLIP and eGFP in PEG solutions in the last subsection. However, this might not be the case for protein diffusion in dextran solutions, where the attractive interaction can be stronger due to possible hydrogen bonding. Intuitively, the "effective" hydrodynamic radius r_h should be larger than r_h^0.

Figure 5 shows two examples of the theoretical results (lines) of the rotational diffusion coefficient, calculated by adopting $r_h = r_h^0$ similar to the case of PEG, one for diffusion of EW-Hb in dextran 500K solution and another for diffusion of F(EW-Hb) in dextran 110K solution. For comparison, the experimental data (symbols) are also presented. Apparently, the theory considerably overestimates the diffusion efficient D_r, indicating that the protein does have an effective hydrodynamic radius larger than r_h^0.

Therefore, it is interesting to apply our model to determine the effective r_h by fitting the experimental data. The results are shown in Figure 6 for available experimental results, where one can see that our theory can show very good agreement with experiment quantitatively. We emphasize that each theoretical curve in this figure is obtained by adjusting one single parameter, i.e., the effective hydrodynamic radius r_h of the protein, while all the other parameters are specified for the system (see Table 2). The values of r_h for different cases are listed in Table 3, where the hydrodynamic radii of protein in pure water r_h^0 are also shown for comparison. Evidently, the effective hydrodynamic radius r_h in dextran solutions is larger than r_h^0 in most cases.

Such excellent fitting with experiments further demonstrates the validity of our basic model, that the diffusion of protein in the system considered here can indeed be modeled as the diffusion of a spherical particle with effective hydrodynamic radius plus the depletion effect.

As already discussed above, the effective hydrodynamic radius r_h should increase with increasing interaction among the protein and the dextran molecules. For EW-Hb, the effective hydrodynamics radius r_h decreases with the increment of R_h of the dextran, as shown in Table 3, indicating a relatively larger interaction among the protein and the polymer molecules. This is also the case for F(EW-Hb), where r_h decreases from 6.21 nm for M_w = 110 kg/mol to 5.7 nm for M_w = 500 kg/mol. Interestingly, for R_h much larger than r_h (the third and fifth lines in Table 3), r_h nearly is equal to r_h^0, indicating that preferential hydration is also applicable in this case.

Figure 7 also implies that not only different protein sizes but also different crowder sizes can modify the diffusion coefficients. Interestingly, the trend in the figure demonstrates

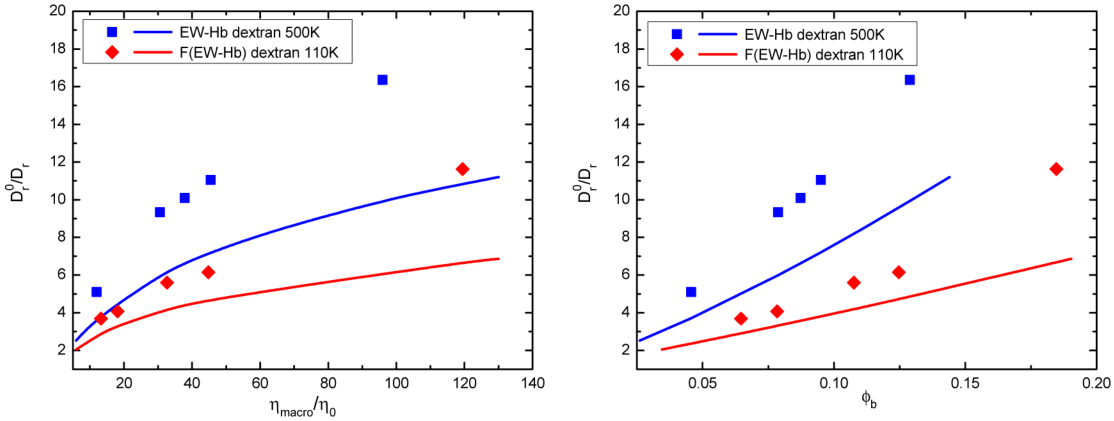

Figure 5. Dependence of relative rotational diffusion coefficient D_r^0/D_r on relative viscosity $\eta_{\mathrm{macro}}/\eta_0$ (left) and that on volume fraction ϕ_b (right), calculated for EW-Hb in dextran 500K (blue line) and F(EW-HB) in dextran 110K (red line), by assuming $r_h = r_h^0$. Symbols are the corresponding experimental data.[9]

DOI: 10.1021/acs.jpcb.6b06248
J. Phys. Chem. B 2016, 120, 10114−10123

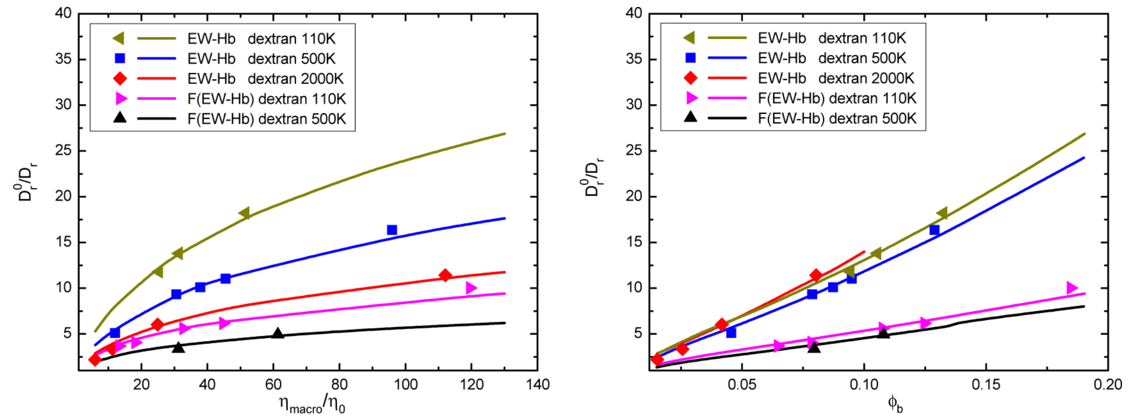

Figure 6. Dependence of relative rotational diffusion coefficients D_r^0/D_r on relative viscosity η_{macro}/η_0 (left) and that on volume fraction ϕ_b (right) calculated for EW-Hb and F(EW-Hb) in dextran solutions, where the corresponding effective hydrodynamic radii r_h are listed in Table 3. Lines are theoretical results, and symbols are experimental data from ref 9.

Table 3. Effective Hydrodynamic Radii r_h for Proteins EW-Hb and F(EW-Hb) in Dextran Solutions[a]

protein	r_h^0 (nm)	dextran M_w (kg/mol)	r_h^0/R_h	r_h (nm)	r_h/r_h^0
EW-Hb	13.4	110	1.72	16.48	1.23
EW-Hb	13.4	500	0.89	15.14	1.13
EW-Hb	13.4	2000	0.48	14.34	1.07
F(EW-Hb)	5.7	110	0.73	6.21	1.09
F(EW-Hb)	5.7	500	0.38	5.7	1.0

[a]The corresponding hydrodynamic radii in pure water r_h^0 are also listed for comparison.

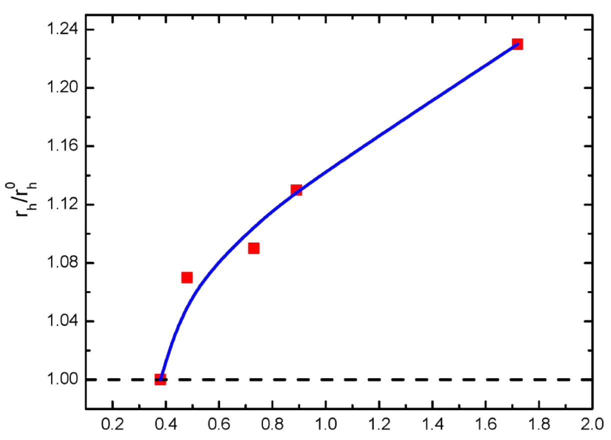

Figure 7. r_h/r_h^0 as a function of the ratio between the hydrodynamic radius of protein in pure water r_h^0 and that of dextran molecules R_h (squares), as listed in Table 3. The line is a hand-drawn curve which indicates the general tendency of the data.

that for larger crowders the steric interaction between protein and crowder is dominant, whereas for smaller crowders the nonspecific interactions (in this case attractive) are important. This issue is very interesting and in line with current debate in the literature concerning the role of interaction beyond hard-core interactions in crowder solutions; see, for example, refs 49 and 50. Generally, solute−water−protein interactions are frequently described in a language of preferential interaction coefficients.[51] For protein diffusion in dextran solutions, there exist two competitive factors that influence the effective hydrodynamic radius r_h of the protein, namely, preferential hydration (PH) and preferential attraction (PA). If PH dominates, the protein will be surrounded by the water molecules and r_h will be nearly r_h^0 as in the case of PEG. If PA dominates, the diffusion of the protein will become slower due to the attractive interaction between the protein and solvent molecule, corresponding to a relatively larger r_h. We note that, in a recent paper,[52] the authors pointed out that nonspecific short-range van der Waals interactions can lead to slowing down of macromolecular diffusion in a cellular environment, which is consistent with the PA picture. For the dextran considered here, the molecule $H(C_6H_{10}O_5)_xOH$ contains three hydroxyls in each segment $[C_6H_{10}O_5]$, and thus may form some hydrogen bonds with the protein. In contrast, the PEG molecule $H(OCH_2CH_2)_nOH$ has no hydroxyl in each segment $[OCH_2CH_2]$, such that the attraction between protein and PEG is weak. Therefore, PH is a reasonable picture for protein diffusion in PEG and $r_h \simeq r_h^0$, while PH and PA may both exist for protein diffusion in dextran. For a given protein, a dextran with smaller R_h may be more competitive to take the position of water molecules, such that it can balance more the PH effect and, as a result, the effective hydrodynamic radius would be larger. Nevertheless, if R_h gets bigger, the protein may be more preferentially surrounded by water and PA becomes dominant such that r_h decreases until it reaches r_h^0.

In Figure 7, we plot the dependence of r_h/r_h^0 as a function of the relative size ratio r_h^0/R_h. r_h increases monotonically with r_h^0/R_h, indicating that PA gets more and more important with decreasing R_h. Nevertheless, the overall size effect is not strong, since r_h/r_h^0 only reaches about 1.23 even for $r_h^0/R_h \sim 1.8$. However, this deviation of r_h from r_h^0 must be taken into account to illustrate the diffusion in dextran, which highlights the effect of PA, as demonstrated in Figures 5 and 6.

■ CONCLUDING REMARKS

In the present work, we have tried to study the diffusion of protein in complex polymer solutions by modeling the protein as a spherical particle with an effective hydrodynamic radius r_h enveloped by a depletion layer, wherein the viscosity varies continuously from that of the pure water solvent η_0 to bulk macroviscosity η_{macro}. The space-dependent viscosity profile $\eta(r)$ in the depletion layer can be calculated by using the scaling theory proposed by Holyst et al., which relates the viscosity profile to the volume fraction distribution $\phi(r)$. We can calculate the hydrodynamic drag force as well as torque exerted to the protein by applying macroscopic fluid mechanics, keeping in mind that η in the standard Navier−Stokes equation

DOI: 10.1021/acs.jpcb.6b06248
J. Phys. Chem. B 2016, 120, 10114−10123

now becomes space-dependent, which then allows us to calculate the translational and rotational diffusion coefficients D_t and D_r numerically. We have used our modeling to study the diffusion of protein in two particular polymer solution systems and then compare the theoretical results with available experimental data. We pay particular attention to how D_t and D_r would depend on the macroscopic viscosity η_{macro} and in to degree the well-known SE relation, i.e., $D_{t,r} \propto \eta_{macro}^{-1}$, is deviated.

The first system we considered is the diffusion of globular proteins in PEG solutions. For this system, the interaction between protein and PEG molecules is weak, such that the protein would be preferentially hydrated. This suggests that the effective hydrodynamic radius r_h, which is required as an input for the model calculation, can be chosen as that in the pure water solvent, r_h^0. All other parameters needed in the model are determined by the polymer solution, here the PEG, and can be obtained from the literature. Remarkably, we find our theoretical results can show very good quantitative agreement with the experimental data. In particular, the interesting finding in the experiments, that the SE relation holds rather well for translational diffusion but SED fails for rotational diffusion, is excellently reproduced. This suggests that our modeling, effective hydrodynamic radius plus depletion layer, has grasped the basic physics of this system, given a correct description of the inhomogeneous viscosity profile.

The other system we considered is about the diffusion of protein in dextran solutions. For this system, a difference from the PEG system is that strong hydrogen bonding may exist between protein and dextran molecules. Therefore, the effective hydrodynamic radius r_h should not simply be r_h^0 in the pure water. To apply our modeling, one must then choose r_h as a fitting parameter. Indeed, we find that our theoretical results with $r_h = r_h^0$ apparently overestimate the diffusion coefficients, indicating that the real r_h should be larger than r_h^0 which is consistent with the picture that the interaction between protein and dextran becomes stronger. Interestingly, we find that all the experimental results, for different solution concentrations, can be reproduced very well by our theoretical framework with a single fitting parameter r_h. This actually further demonstrates that our basic modeling, rewritten here again, effective hydrodynamic radius plus depletion layer, works well for this system. We have also investigated how r_h changes with the relative size of the protein to the dextran molecule, showing that r_h/r_h^0 increases monotonically with r_h^0/R_h.

Here are some discussions about our modeling. First, one should note that the viscosity profile here we described is actually "macroscopic" rather than the microviscosity. Although the depletion layer may be of small depth, here $\eta(r)$ describes a macroscopic viscosity in the mean-field level. Second, here we have applied the scaling theory for macroscopic viscosity proposed by Holyst et al., which was proven to be correct in many complex solution systems. One may use simple theories such as the Huggins or Martin formulas to describe the scaling of viscosity with concentration; however, quantitative agreements with the experiments as demonstrated in our present work would not be available (not shown). Finally, our model surely has its range of validity. For instance, the volume fraction profile $\phi(r)$ is obtained by standard depletion theory near a flat wall and then extended to a spherical particle. Such a formula may become incorrect if the solute size is too small compared to the solvent. If the solute size is much larger than the solvent, the depletion layer would actually disappear, the viscosity would become homogeneous, and the SE and SED relations would hold for D_t and D_r, respectively.

In summary, we have proposed a basic model to understand the translational and rotational diffusion behavior of proteins in complex polymer solutions, by combining macroscopic fluid mechanics with scaling theory of macroscopic viscosity as well as depletion theory. The theory can well reproduce the diffusion behaviors of some proteins in PEG and dextran solutions and help in understanding the decoupling of translational and rotational diffusion observed experimentally. Since diffusion of proteins in complex solutions is of ubiquitous importance in many systems, our study may find many applications and open more perspectives in relevant research fields.

■ AUTHOR INFORMATION

Corresponding Authors

*E-mail: zhaonanr@scu.edu.cn.
*E-mail: hzhlj@ustc.edu.cn.

Notes

The authors declare no competing financial interest.

■ ACKNOWLEDGMENTS

This work was supported by National Natural Science Foundation of China (Grant Nos. 21373141 and 21473165).

■ REFERENCES

(1) Pederson, T. Diffusional Protein Transport Within the Nucleus: A Message in the Medium. *Nat. Cell Biol.* **2000**, *2*, E73−E74.
(2) Cluzel, P.; Surette, M.; Leibler, S. An Ultrasensitive Bacterial Motor Revealed by Monitoring Signaling Proteins in Single Cells. *Science* **2000**, *287*, 1652−1655.
(3) Macnab, R. M. Action at a Distance-Bacterial Flagellar Assembly. *Science* **2000**, *290*, 2086−2087.
(4) Guthold, M.; Zhu, X.; Rivetti, C.; Yang, G.; Thomson, N. H.; Kasas, S.; Hansma, H. G.; Smith, B.; Hansma, P. K.; Bustamante, C. Direct Observation of One-Dimensional Diffusion and Transcription by Escherichia Coli RNA Polymerase. *Biophys. J.* **1999**, *77*, 2284−2294.
(5) Berry, H. Monte Carlo Simulations of Enzyme Reactions in Two Dimensions: Fractal Kinetics and Spatial Segregation. *Biophys. J.* **2002**, *83*, 1891−1901.
(6) Struntz, P.; Weiss, M. Multiplexed Measurement of Protein Diffusion in Caenorhabditis Elegans Embryos with SPIM-FCS. *J. Phys. D: Appl. Phys.* **2016**, *49*, 044002.
(7) Kozer, N.; Kuttner, Y. Y.; Haran, G.; Schreiber, G. Protein-Protein Association in Polymer Solutions: From Dilute to Semidilute to Concentrated. *Biophys. J.* **2007**, *92*, 2139−2149.
(8) Busch, N. A.; Kim, T.; Bloomfield, V. A. Tracer Diffusion of Proteins in DNA Solutions. 2. Green Fluorescent Protein in Crowded DNA Solutions. *Macromolecules* **2000**, *33*, 5932−5937.
(9) Lavalette, D.; Tétreau, C.; Tourbez, M.; Blouquit, Y. Microscopic Viscosity and Rotational Diffusion of Proteins in a Macromolecular Environment. *Biophys. J.* **1999**, *76*, 2744−2751.
(10) Tabaka, M.; Kalwarczyk, T.; Szymanski, J.; Hou, S.; Holyst, R. The Effect of Macromolecular Crowding on Mobility of Biomolecules, Association Kinetics,and Gene Expression in Living Cells. *Front. Phys.* **2014**, *2*, 54.
(11) Kozer, N.; Schreiber, G. Effect of Crowding on Protein-Protein Association Rates: Fundamental Differences between Low and High Mass Crowding Agents. *J. Mol. Biol.* **2004**, *336*, 763−774.
(12) Kuttner, Y. Y.; Kozer, N.; Segal, E.; Schreiber, G.; Haran, G. Separating the Contribution of Translational and Rotational Diffusion to Protein Association. *J. Am. Chem. Soc.* **2005**, *127*, 15138−15144.
(13) Schreiber, G.; Haran, G.; Zhou, H. Fundamental Aspects of Protein-Protein Association Kinetics. *Chem. Rev.* **2009**, *109*, 839.

DOI: 10.1021/acs.jpcb.6b06248
J. Phys. Chem. B 2016, 120, 10114−10123

(14) Sherman, E.; Itkin, A.; Kuttner, Y. Y.; Rhoades, E.; Amir, D.; Haas, E.; Haran, G. Using Fluorescence Correlation Spectroscopy to Study Conformational Changes in Denatured Proteins. *Biophys. J.* **2008**, *94*, 4819−4827.
(15) Grabowski, C. A.; Mukhopadhyay, A. Size Effect of Nanoparticle Diffusion in a Polymer Melt. *Macromolecules* **2014**, *47*, 7238−7242.
(16) Li, C.; Wang, Y.; Pielak, G. J. Translational and Rotational Diffusion of a Small Globular Protein under Crowded Conditions. *J. Phys. Chem. B* **2009**, *113*, 13390−13392.
(17) Wang, Y.; Li, C.; Pielak, G. J. Effects of Proteins on Protein Diffusion. *J. Am. Chem. Soc.* **2010**, *132*, 9392−9397.
(18) Kohli, I.; Mukhopadhyay, A. Contrasting Nanoparticle Diffusion in Branched Polymer and Particulate Solutions: More Than Just Volume Fraction. *Soft Matter* **2013**, *9*, 8974−8979.
(19) Kohli, I.; Mukhopadhyay, A. Diffusion of Nanoparticles in Semidilute Polymer Solutions: Effect of Different Length Scales. *Macromolecules* **2012**, *45*, 6143−6149.
(20) Liu, J.; Cao, D.; Zhang, L. Molecular Dynamics Study on Nanoparticle Diffusion in Polymer Melts: A Test of the Stokes-Einstein Law. *J. Phys. Chem. C* **2008**, *112*, 6653−6661.
(21) Egorov, S. A. Anomalous Nanoparticle Diffusion in Polymer Solutions and Melts: A Mode-Coupling Theory Study. *J. Chem. Phys.* **2011**, *134*, 084903.
(22) Tuteja, A.; Mackay, M. E.; Narayanan, S.; Asokan, S.; Wong, M. S. Breakdown of the Continuum Stokes-Einstein Relation for Nanoparticle Diffusion. *Nano Lett.* **2007**, *7*, 1276−1281.
(23) Holyst, R.; Bielejewska, A.; Szymański, J.; Wilk, A.; Patkowski, A.; Gapiński, J.; Żywociński, A.; Kalwarczyk, T.; Kalwarczyk, E.; Tabaka, M.; et al. Scaling Form of Viscosity at All Length-Scales in Poly(Ethylene Glycol) Solutions Studied by Fluorescence Correlation Spectroscopy and Capillary Electrophoresis. *Phys. Chem. Chem. Phys.* **2009**, *11*, 9025−9032.
(24) Kalwarczyk, T.; Zięba̧cz, N.; Bielejewska, A.; Zaboklicka, E.; Koynov, K.; Szymański, J.; Wilk, A.; Patkowski, A.; Gapiński, J.; Butt, H.; et al. Comparative Analysis of Viscosity of Complex Liquids and Cytoplasm of Mammalian Cells at the Nanoscale. *Nano Lett.* **2011**, *11*, 2157−2163.
(25) Zięba̧cz, N.; Wieczorek, S. A.; Kalwarczyk, T.; Fiałkowski, M.; Holyst, R. Crossover Regime for the Diffusion of Nanoparticles in Polyethylene Glycol Solutions: Influence of the Depletion Layer. *Soft Matter* **2011**, *7*, 7181−7186.
(26) Kalwarczyk, T.; Sozanski, K.; Ochab-Marcinek, A.; Szymanski, J.; Tabaka, M.; Hou, S.; Holyst, R. Motion of Nanoprobes in Complex Liquids Within the Framework of the Length-Scale Dependent Viscosity Model. *Adv. Colloid Interface Sci.* **2015**, *223*, 55−63.
(27) Wiśniewska, A.; Sozański, K.; Kalwarczyk, T.; Kȩdra-Królik, K.; Pieper, C.; Wieczorek, S. A.; Jakieła, S.; Kȩdra-Królik, K.; Pieper, C.; Wieczorek, S. A.; et al. Scaling of Activation Energy for Macroscopic Flow in Poly(Ethylene Glycol) Solutions: Entangled-Non-Entangled Crossover. *Polymer* **2014**, *55*, 4651−4657.
(28) Sozański, K.; Wiśniewska, A.; Kalwarczyk, T.; Holyst, R. Activation Energy for Mobility of Dyes and Proteins in Polymer Solutions: From Diffusion of Single Particles to Macroscale Flow. *Phys. Rev. Lett.* **2013**, *111*, 228301.
(29) Lavalette, D.; Hink, M. A.; Tourbez, M.; Tétreau, C.; Visser, A. J. Proteins as Micro Viscosimeters: Brownian Motion Revisited. *Eur. Biophys. J.* **2006**, *35*, 517−522.
(30) Fan, T.-H.; Xie, B.; Tuinier, R. Asymptotic Analysis of Tracer Diffusivity in Nonadsorbing Polymer Solutions. *Phys. Rev. E* **2007**, *76*, 051405.
(31) Fan, T.-H.; Dhont, J. K. G.; Tuinier, R. Motion of a Sphere Through a Polymer Solution. *Phys. Rev. E* **2007**, *75*, 011803.
(32) Tuinier, R.; Dhont, J. K. G.; Fan, T. How Depletion Affects Sphere Motion Through Solutions Containing Macromolecules. *Europhys. Lett.* **2006**, *75*, 929−935.
(33) Chong, S.-H.; Kob, W. Coupling and Decoupling Between Translational and Rotational Dynamics in a Supercooled Molecular Liquid. *Phys. Rev. Lett.* **2009**, *102*, 025702.
(34) Edmond, K. V.; Elsesser, M. T.; Hunter, G. L.; Pine, D. J.; Weeks, E. R. Decoupling of Rotational and Translational Diffusion in Supercooled Colloidal Fluids. *Proc. Natl. Acad. Sci. U. S. A.* **2012**, *109*, 17891−17896.
(35) Tabaka, M.; Sun, L.; Kalwarczyk, T.; Holyst, R. Implications of Macromolecular Crowding for Protein-Protein Association Kinetics in the Cytoplasm of Living Cells. *Soft Matter* **2013**, *9*, 4386−4389.
(36) Bhat, R.; Timasheff, S. N. Steric Exclusion is the Principal Source of the Preferential Hydration of Proteins in the Presence of Polyethylene Glycols. *Protein Sci.* **1992**, *1*, 1133−1143.
(37) Fleer, G. J.; Skvortsov, A. M.; Tuinier, R. Mean-Field Equation for the Depletion Thickness. *Macromolecules* **2003**, *36*, 7857−7872.
(38) Huggins, M. L. Solutions of Long Chain Compounds. *J. Chem. Phys.* **1941**, *9*, 440.
(39) Fleer, G. J.; Skvortsov, A. M. Theory for Concentration and Solvency Effects in Size-Exclusion Chromatography of Polymers. *Macromolecules* **2005**, *38*, 2492−2505.
(40) Tuinier, R.; Fan, T.-H. Scaling of Nanoparticle Retardation in Semi-Dilute Polymer Solutions. *Soft Matter* **2008**, *4*, 254−257.
(41) Cai, L.-H.; Panyukov, S.; Rubinstein, M. Hopping Diffusion of Nanoparticles in Polymer Matrices. *Macromolecules* **2015**, *48*, 847−862.
(42) Saffman, P. G.; Delbrück, M. Brownian Motion in Biological Membranes. *Proc. Natl. Acad. Sci. U. S. A.* **1975**, *72*, 3111−3113.
(43) Halle, B.; Davidovic, M. Biomolecular Hydration: FromWater Dynamics to Hydrodynamics. *Proc. Natl. Acad. Sci. U. S. A.* **2003**, *100*, 12135−12140.
(44) Linegar, K. L.; Adeniran, A. E.; Kostko, A. F.; Anisimov, M. A. Hydrodynamic Radius of Polyethylene Glycol in Solution Obtained by Dynamic Light Scattering. *Colloid J.* **2010**, *72*, 279−281.
(45) Dong, Y.; Feng, X.; Zhao, N.; Hou, Z. Diffusion of Nanoparticles in Semidilute Polymer Solutions: A Mode-Coupling Theory Study. *J. Chem. Phys.* **2015**, *143*, 024903.
(46) Venturoli, D.; Rippe, B. Ficoll and Dextran vs. Globular Proteins as Probes for Testing Glomerular Permselectivity: Effects of Molecular Size, Shape, Charge, and Deformability. *Am. J. Physiol.* **2005**, *288*, F605−F613.
(47) Banks, D. S.; Fradin, C. Anomalous Diffusion of Proteins Due to Molecular Crowding. *Biophys. J.* **2005**, *89*, 2960−2971.
(48) Kotagiri, N.; Kim, J. W. Carbon Nanotubes Fed on "Carbs": Coating of Single-Walled Carbon Nanotubes by Dextran Sulfate. *Macromol. Biosci.* **2010**, *10*, 231−238.
(49) Sukenik, S.; Sapir, L.; Harries, D. Balance of Enthalpy and Entropy in Depletion Forces. *Curr. Opin. Colloid Interface Sci.* **2013**, *18*, 495−501.
(50) Sapir, L.; Harries, D. Is the Depletion Force Entropic? Molecular Crowding Beyond Steric Interactions. *Curr. Opin. Colloid Interface Sci.* **2015**, *20*, 3−10.
(51) Parsegian, V. A. Protein-Water Interactions. *Int. Rev. Cytol.* **2002**, *215*, 1−31.
(52) Ando, T.; Skolnick, J. Crowding and Hydrodynamic Interactions Likely Dominate in Vivo Macromolecular Motion. *Proc. Natl. Acad. Sci. U. S. A.* **2010**, *107*, 18457−18462.

DOI: 10.1021/acs.jpcb.6b06248
J. Phys. Chem. B 2016, 120, 10114−10123